RESEARCH ARTICLE OPEN ACCESS

Evaluation of Flat-Plate Solar Thermal Collector Daily Utilizability for Some Nigerian Cities

Njoku M.C.[*], Nwaji G.N.[**], Ofong I.[**], Ogueke N.V.[**], and Anyanwu E.E.[**]
[*]*Department of Mechanical Engineering, Federal Polytechnic, Nekede, P.M.B. 1036 Owerri, Imo-State, Nigeria*
[**]*Department of Mechanical Engineering, Federal University of Technology, P.M.B. 1526 Owerri, Imo-State, Nigeria*
Corresponding author: Njoku M.C

ABTRACT
Evaluation of flat plate solar thermal collector daily utilizability for some Nigerian cities has been carried out using monthly average clearness index values estimated from measured daily solar radiation of twelve years data (1975 – 1986). Six study locations which include Abuja, Bauchi, Benin-City, Kano, Lagos and Owerri were selected from each geo-political zone of Nigeria. Utilizability curves were drawn by linear curve fitting of the distribution curves of the monthly average clearness index for each study location. Monthly average clearness index of higher values which are common during the dry season have been shown to yield more utilizability values, indicating the possibility of harvesting more solar radiation in such locations. The utilizability values estimated for each study location may therefore be used for locations with similar meteorological characteristic in the tropics.

Keywords: clearness index, cumulative frequency curves, solar thermal collector, solar radiation, utilizability

---

Date of Submission: 28-01-2020 Date Of Acceptance: 09-02-2020

I. INTRODUCTION

The availability of abundant solar energy makes it a viable source of energy resources in Nigeria for domestic and industrial usage [1]. Harnessing solar energy for useful purposes requires solar thermal collectors of which the flat plate solar thermal collectors are commonly used for low temperature application such as air-conditioning, space and domestic water heating requirements.

A flat plate solar thermal collector has been the traditional device for solar thermal collection for decades and is most commonly utilized for domestic water and space heating. They have the following advantages (i) they do not require tracking of the sun, (ii) inexpensive to construct, (iii) mechanically simple to operate and (iv) require low maintenance. Based on the heat transfer fluid used, flat plate solar collector may be classified into two types [2]: the air type and liquid type. The air type of flat plate solar collector uses air as the heat transfer medium during operation of the collector. It is typified by low heat capacity, high flow rate and large dimensions [3]. Its applications are found in the drying of agricultural produce and residential heating and cooling of ventilated air in buildings. The convectional working fluid of the liquid type flat plate solar thermal collector is water, glycol and oil [4]. Its application is commonly found in water heating, refrigeration, etc.

Flat-plate solar thermal collectors are made up of a flat metallic plate, painted black on the side facing the sun to maximize the absorption of solar radiation incident on it, (thereby acting as the heat collector) and insulated on the underside and edges to prevent/reduce heat losses. On top of and parallel to the black painted flat metallic plate collector are mounted one or more transparent glazing material which transmits the short-wave solar radiation to the collector plate but opaque to long-wave solar radiation from the collector plate. The transparent glazing material is usually placed a distance of 25 – 35 mm from the collector plate [5]. Provision is made to remove the energy absorbed in the collector absorber plate by circulating either air through an air space below the collector plate or water through tubes soldered to the collector plate
Generally, the performance evaluation of flat-plate solar thermal collector is often measured in terms of instantaneous or peak efficiency based on clear day and quantity of incident solar radiation the solar thermal collector is capable of receiving. However, as a result of the irregular behaviour of weather condition, there is need to determine the long term useful energy delivery over all weather conditions. The essence is to predict correctly the optimal performance, economic evaluation and

maintenance requirement of solar thermal collector before installation.

Two common methods employed for the estimation of the long term performance of solar thermal collectors include simulation method with the aid of Transient System Simulation (TRNSYS) method which presents many advantages [6], though, it requires money and expertise before a useful result is obtained [7]; and the use of a design method which includes the f-chat and utilizability method. The f-chat method is limited to a specific system for which it is developed. The utilizability method first developed by [8] and later generalized by [9] is the fraction of the total solar radiation incident on a surface which exceeds a specified intensity called the critical radiation. This method is handy and yield results with relatively little efforts but at the expense of a certain amount of accuracy [10].

Several researchers have presented mathematical correlations for the estimation of utilizability. Ref. [7] used the generalized curves of [9] to develop correlations for the evaluation of utilizability values for any given location. Ref. [11] later used twenty years of hourly data to prove that correlation developed by Ref. [7] from the generalized curves of Ref. [9] is inaccurate for most temperate locations. Ref. [12] developed a simple algorithm for evaluating the hourly utilizability function. Ref. [13] developed correlations for prediction of total energy that can be delivered by solar collector of different configurations. Ref. [14] from the analysis of one minute solar radiation data in Pert, Australia have shown that the cumulative frequency curves generated took a different pattern from those of Ref. [9]. Ref. [15] reported that these correlations for computing utilizability are based on data obtained from United State of America weather which is a temperate region and may not be appropriate for tropical region like Nigeria.

Thus, Ref. [16] used the data of Bet Dagan, Israel to demonstrate the difference between hourly versus daily insolation. Ref. [17] determined utilizability function for several locations in Spain. Ref. [18] used the utilizability function on PV water pumping system. In Hong Kong, Ref. [19] used the utilizability function to predict the performance of solar collectors. Ref. [20] studied for two different locations in South India using global radiation data from their locations. In another study, Ref. [21] presented monthly mean daily utilizability of South India. Ref. [22] studied utilizability for three cities in India. Ref. [10] presented for a city in Pakistan. Ref. [23] studied the long term performance of double slope tilted-wick type solar still using utilizability method. In this study, evaluation of daily utilizability for flat plate solar collector is carried out for some selected cities in Nigeria using measured daily solar radiation data from the study locations.

II. METHOD

Materials

Six cities, one from each geopolitical region of Nigeria are selected for this study. The latitude, longitude and elevation of the study locations are given in Table 1. Twelve years (1975 - 1986) of measured daily global solar radiation for each city was sourced from Nigerian Building and Road Research Institute (NBRRI).

Table 1 selected cities with longitude, latitude and elevation

Cities	Latitude	Longitude	Elevation
Abuja	9.40^{o}N	6.29^{o}E	319m
Bauchi	10.30^{o}N	10.00^{o}E	458m
Benin City	6.32^{o}N	5.62^{o}E	135m
Kano	12.00^{o}N	8.31^{o}E	456m
Lagos	6.58^{o}N	3.75^{o}E	73m
Owerri	5.49^{o}N	7.03^{o}E	176m

Energy Balance of Flat Plate Collectors

Under steady-state condition, the performance of a flat plate solar collector can be described by an energy balance that indicates the distribution of incident solar radiation into useful energy gain and heat energy loss. Hence, the rate of useful heat energy gain (q_u) by a flat plate solar collector is the difference between the rate at which solar energy is absorbed by the absorber plate (q_{ab}) and the rate at which heat energy is lost to the surrounding (q_L) due to temperature difference between the absorber plate and the ambient. This may be stated mathematically as:

$$q_u = q_{ab} - q_L \qquad (1)$$

The useful energy absorbed by the solar collector is expressed as:

$$q_{ab} = A_c(\tau\alpha)I \qquad (2)$$

Where A_c is the area of the solar collector, $\tau\alpha$ is the transmittance-absorptance product, and I is the hourly incident global solar radiation on a horizontal surface.

While, the collector energy losses is expressed as:

$$q_L = U_L A_c(T_{in} - T_a) \qquad (3)$$

where U_L is the overall heat loss coefficient, T_a is the ambient temperature and T_{in} is the fluid inlet temperature.
Substituting Eq. (2) and (3) into Eq. (1) yields

$$Q_u = A_C F_R[I(\tau\alpha) - U_L(T_{in} - T_a)] \quad (4)$$

Eq. (4) is known as the Hottel–Whiller-Bliss (HWB) equation. It is an excellent tool for understanding the implications of design changes to the solar collector. As an instantaneous equation, in this form, it is not particularly useful in estimating the long-term performance of a solar energy system [24]. One useful tool to tackle this challenge is the concept of solar thermal collector utilizability.

Thus, to relate utilizability factor with useful energy gained, the concept of stagnation temperature in solar collector is used. Assuming a stagnation temperature condition during which the solar thermal collector absorber plate cannot sufficiently transfer the useful energy to the working fluid. The stagnation period occurs under no flow condition, and the collector plate and fluid are taken as having the same temperature [22]. Thus, the useful energy gained by the solar thermal collector is taken as zero($Q_u = 0$), during stagnation period. Hence, under stagnation conditions:

$$A_c F_R(\tau\alpha)I = U_L A_c F_R(T_{in} - T_a) \quad (5)$$

Also at the stagnation point, the total hourly incident global solar radiation on the collector is taken to be the critical solar radiation i.e. $I = I_C$. Therefore,

$$A_c F_R(\tau\alpha)I_C = U_L A_c F_R(T_{in} - T_a) \quad (6)$$

Thus, for a flat plate solar collector under stagnation condition, the critical solar radiation can be expressed as:

$$I_C = \frac{U_L(T_{in} - T_a)}{(\tau\alpha)} \quad (7)$$

Dividing Eq. (4) through by $(\tau\alpha)$, gives

$$\frac{Q_u}{(\tau\alpha)} = A_c F_R\left[I - \frac{U_L(T_{in} - T_a)}{(\tau\alpha)}\right] \quad (8)$$

Substituting Eq. (7) into Eq. (8) yields:

$$Q_u = F_R A_c(\tau\alpha)[I - I_C] \quad (9)$$

Eq. (9) is still an instantaneous expression. The monthly average daily global solar radiation data on a horizontal surface ($\bar{H}$) obtained can be converted to monthly average global values by division by the period of solar radiation availability for a given location, covering sunrise and sunset. Theoretically, a 12 hour period spans sunrise and sunset in the present study location. Hence, the monthly average global solar radiation on a horizontal surface, designated as $\bar{I}_m$ can be expressed as:

$$\bar{I}_m = \frac{\bar{H}}{12} \quad (10)$$

For an hour, the average rate of total solar radiation incident on the solar collector has to be used to determine the long term performance per hour. Thus, dividing Eq. (9) by Eq. (10), for the average monthly global radiation, per unit area, gives

$$Q_u = F_R(\tau\alpha)\left[\frac{(I - I_C)}{\bar{I}_m}\right] \quad (11)$$

While, the long-term average useful energy the solar thermal collector is capable of collecting for i-th hour (i.e. 10-11am) of the day, averaged over N days is

$$Q_u = F_R(\tau\alpha)\frac{1}{N}\sum^N\left[\frac{(I - I_C)}{\bar{I}_m}\right]^+ \quad (12)$$

The positive sign indicates that only positive values of an hourly utilizability factor are considered.
The hourly collector utilizability factor for an hour of each day in terms of critical radiation is given by [25] as:

$$\phi = \frac{1}{N}\sum^N\left[\frac{(I - I_C)}{\bar{I}_m}\right]^+ \quad (13)$$

Where ϕ is the daily utilizability.

In terms of critical radiation ratio, the hourly utilizability factor of Eq. (13) can be written as

$$\phi = \frac{1}{N}\sum^N(X - X_C)^+ \quad (14)$$

Where X is the radiation ratio, which can be expressed as:

$$X = \frac{I}{\bar{I}_m} \quad (15)$$

and

$$X_c = \frac{I_c}{\bar{I}_m} \quad (16)$$

According to [20], the daily utilizability (ϕ) from hourly cumulative frequency curves can be expressed as:

$$\phi = \int_X^{X_{max}}(1 - f)dX \quad (17)$$

Eq. (16) can be transformed to take the form of Eq. (17) by modifying the limits of integration:

$$\phi = 1 - \int_0^X X df - (1 - f) dX \qquad (18)$$

Where f is the fractional time which can be correlated with X using linear curve fitting techniques at given clearness indices.

For instance, from Table 2e, the linear equation for Owerri at clearness index of 0.52 is:

$$f = 0.385 + 1.228X \qquad (19)$$

Tables 2(a-f) show the monthly utilizability values for each study location.

a. abuja

K_T	(f)	ϕ
0.63	$0.358 + 1.283X$	$1 - 0.642X_c + 0.642X_c^2$
0.57	$0.673 + 0.652X$	$1 - 0.327X_c + 0.326X_c^2$
0.53	$0.687 + 0.624X$	$1 - 0.313X_c + 0.312X_c^2$
0.45	$0.522 + 0.955X$	$1 - 0.478X_c + 0.478X_c^2$

b. Lagos

K_T	(f)	ϕ
0.56	$0.393 + 1.213X$	$1 - 0.607X_c + 0.607X_c^2$
0.53	$0.370 + 1.258X$	$1 - 0.630X_c + 0.629X_c^2$
0.40	$0.411 + 1.177X$	$1 - 0.589X_c + 0.589X_c^2$
0.46	$0.420 + 1.158X$	$1 - 0.580X_c + 0.579X_c^2$
0.56	$0.234 + 1.531X$	$1 - 0.766X_c + 0.766X_c^2$

c. Bauchi

K_T	(f)	ϕ
0.63	$0.458 + 1.082X$	$1 - 0.542X_c + 0.227X_c^2$
0.53	$0.441 + 1.116X$	$1 - 0.559X_c + 0.555X_c^2$
0.48	$0.540 + 0.918X$	$1 - 0.46X_c + 0.459X_c^2$

d. Kano

K_T	(f)	ϕ
0.63	$0.699 + 0.602X$	$1 - 0.301X_c + 0.301X_c^2$
0.53	$0.668 + 0.663X$	$1 - 0.332X_c + 0.332X_c^2$
0.54	$0.569 + 0.862X$	$1 - 0.431X_c + 0.431X_c^2$

e. Owerri

K_T	(f)	ϕ
0.56	$0.485 + 1.029X$	$1 - 0.515X_c + 0.515X_c^2$
0.52	$0.385 + 1.228X$	$1 - 0.615X_c + 0.614X_c^2$
0.38	$0.250 + 1.499X$	$1 - 0.750X_c + 0.750X_c^2$
0.45	$0.506 + 0.987X$	$1 - 0.494X_c + 0.495X_c^2$
0.49	$0.357 + 1.266X$	$1 - 0.643X_c + 0.633X_c^2$

f. Benin City

K_T	(f)	ϕ
0.55	$0.538 + 0.921X$	$1 - 0.462X_c + 0.461X_c^2$
0.51	$0.555 + 0.887X$	$1 - 0.445X_c + 0.444X_c^2$
0.38	$0.401 + 1.170X$	$1 - 0.599X_c + 0.585X_c^2$
0.41	$0.363 + 1.240X$	$1 - 0.637X_c + 0.620X_c^2$
0.46	$0.440 + 1.119X$	$1 - 0.560X_c + 0.560X_c^2$
0.34	$0.250 + 1.499X$	$1 - 0.750X_c + 0.750X_c^2$

By substituting Eq. (19) into Eq. (18) and performing the integration to the limit of the critical radiation ratio, the daily utilizability function for a horizontal surface is obtained. Thus,

$$\phi = 1 - 0.615X_c + 0.614X_c^2 \qquad (20)$$

By using the above procedure, the cumulative frequency distribution curves for each clearness index for all the study locations are drawn.

Once the daily utilizability values are known, the monthly useful energy delivered by a flat plate collector per unit area can be obtained from the following equation

$$Q_u = F_R(\tau\alpha)\phi N\overline{H} \qquad (21)$$

Clearness Index

The condition of the sky during a given period or month can be determined by the clearness index (K_T). Since K_T is a ratio, it is a dimensionless parameter which represents the fraction of the extraterrestrial radiation transmitted through the atmosphere. The clearness index is given as

$$K_T = \frac{\bar{H}}{H_O} \qquad (22)$$

Where H_o and $\bar{H}$ are monthly extraterrestrial radiation and monthly average daily total radiation on a horizontal surface, respectively. The monthly mean daily extraterrestrial radiation for the study locations is given as by [25]

$$H_O = \frac{24\ x3600G_{sc}}{\pi}\left(1 + 0.033cos\frac{360n}{365}\right)x\left(cos\emptyset cos\delta sin\omega_s + \frac{\pi\omega_s}{180}sin\emptyset sin\delta\right) \qquad (23)$$

Where G_{sc} is solar constant given as 1367W/m^2, $\emptyset$ is the location latitude, δ is the declination angle and ω_s is the hour angle at sunset.

The angle of declination (δ) in degree for any day of the year is the angle between the line joining the centers of the sun and the earth and its projection on the equatorial plane and can be calculated as by [26]:

$$\delta = 23.45\ sin\left(360\ \frac{284+n}{365}\right) \qquad (24)$$

Where (n) is the average day for each month
The sunset hour angle (ω_s) can be calculated as by [25]:

$$\omega_s = cos^{-1}(-tan\emptyset\ tan\delta) \qquad (25)$$

III. RESULTS AND DISCUSSION

The flat-plate solar collector employed for sample performance comprises of an aluminum substrate painted black. The absorber plate area is 1.2m^2 with a thickness of 0.005m. A glass cover of 0.002m thickness was placed 0.03m above the plate. While, collector heat removal factor, transmissivity-absorptivity product and overall heat loss coefficient of 0.776, 0.84 and 6.95Wm^{-2o}C^{-1}, respectively were estimated for the solar thermal collector.

In Nigeria, the seasonal period is divided into two: the rain and dry seasons. The period of rain season consists of the following months; May, June, July, August September and October during which each part of the country experiences different levels of rainfall. The months of November, December, January, February, March and April make up the dry season during which dry and dusty wind from the Sahara desert blows across the country.

Table 3 shows the seasonal classification of clearness index (K_T) value for the six chosen study locations. Following the works of Ref [27] and [28], the monthly K_T values for each city is grouped according to the closeness of their values and their monthly average. For Abuja, the seasonal periods are classified into four groups. Two groups are identified in the dry season, where the months of November, December, January, February and March are grouped together with a monthly average K_T value of 0.63 and the second group of the dry season consists of April only with a monthly average K_T value of 0.57. For the Rainy season period in Abuja, the months of May, June and October are grouped together while the months of July, August and September formed another group with monthly average K_T values of 0.53 and 0.44 respectively for each of the groups.

The city of Lagos followed a different trend; two and three groups are identified in the dry and the rain season, respectively. For the dry season period, the first group consists of the months of December, January, and February while the second group has the months of November, March and April. Each group of the dry season period in the city of Lagos has a monthly average K_T values of 0.56 and 0.53, respectively. In the rainy season, the first group consists of the months of June, July, August and September with an average monthly K_T value of 0.40. The second and third groups during the rainy season for the city of Lagos are made up of the months of May and October, respectively with an average monthly K_T values of 0.46 and 0.56. For the city of Bauchi, a total of three groups where observed. One and two groups are observed for the dry and rain season, respectively. All the months of the dry season with an average monthly K_T value of 0.63 were grouped together. For the rainy period in Bauchi, two groups are identified. The first group consists of May, June, July, September and October with an average monthly K_T value of 0.53. The second group has the month of August with an average monthly K_T value of 0.48.

For the city of Kano, a similar trend in Bauchi is observed. All the months of the dry season period are grouped into one seasonal period with an average monthly K_T value of 0.63, while the rainy season period have two groups. The first group consists of April, May, and June with an average monthly K_T value of 0.61. The months of June, August and September make up the second

group with an average monthly K_T value of 0.54. For the city of Owerri, a total of five groups are identified for the two seasonal periods. The dry season consists of two groups, November, December and January with an average monthly K_T of 0.56, represents the first group. The second group in the dry season consists of the months of February, March and April with an average monthly K_T of 0.52. The rainy season for Owerri, has a total of three groups with the months of July, August and September forming the first group with an average monthly K_T value of 0.38. The second group consists of the months of October and June with an average monthly K_T value of 0.45 and the month May recorded an average monthly K_T value of 0.49 which forms the third group. Six periods are identified for Benin City. The dry season has two seasonal periods. The first group for the dry season period is made up of the months of November, December and January with an average monthly K_T value of 0.55 while the second group in the dry season consists of the months of February, March and April with an average monthly K_T value of 0.51. The rainy season consist of four groups. The months of July and September form the first group with an average monthly K_T value of 0.38. The months of June and October with an average monthly K_T value of 0.41 form the second group. The third and fourth groups consist of the month of May and August, respectively, with an average monthly clearness index of 0.46 and 0.34.

The six seasonal patterns identified for Benin City seem to be in line with the finding of Ref. [28] for Ibadan which is within the same geographical belt. In the same vein, the five seasonal patterns identified for Owerri and Lagos coincide with the findings of Ref. [27] for Port Harcourt, Nigeria. These three cities may be said to have similar meteorological conditions because of the closeness to the ocean. It is observed that Abuja, Bauchi and Kano recorded four, three and three seasonal patterns, respectively. The cities of Abuja, Bauchi and Kano are located in the Northern part of Nigeria and are known for high level of sunshine as a result of their closeness to the Sahara desert; Kano and Bauchi being the closest.

Different researchers have adopted different K_T values to characterize their local sky conditions. For example, Ref. [29] proposed $K_T > 0.2$ and $K_T < 0.6$ for cloudy and clear sky, respectively. Ref. [30] and [31] used K_T values of 0 – 0.15, > 0.15 – 0.7 and > 0.7 for overcast, partly cloudy and clear skies respectively and Ref. [27] used $0.12 \leq K_T \leq 0.35$ and $K_T > 0.65$ for cloudy and clear days, respectively. A large value of K_T indicates a clear atmosphere of low turbidity and cloudiness and a small value of K_T indicates an overcast atmosphere of high turbidity and cloudiness. Using the range given by Ref. [27], it can be seen from Table 3 that the monthly average K_T values range from 0.34 – 0.63 for all the study locations. Thus, there is no clear day i.e. $K_T \geq 0.65$ recoded for any of the study locations. During the dry season, all the days of the month can be said to be partly cloudy for all the study locations. It is seen from Table 3 that the worst seasonal periods occur during the rainy season for all the study locations. This is expected as a result of the overcast weather condition that is common during the rainy season in Nigeria.

Table 3 seasonal classification of clearness index (K_T) value

K_T Values								
Period	Abuja		Period	Lagos		Period	Bauchi	
	Ind.	**Ave**		Ind.	**Ave**		Ind.	**Ave**
Dry Season			**Dry Season**			**Dry Season**		
a. Nov, Dec, Jan, Feb, Mar,	0.63, 0.65 0.63,	**0.63**	**a**. Dec, Jan, Feb	0.57, 0.56	**0.56**	**a**. Nov, Dec, Jan, Feb, Mar, April	0.62, 0.63, 0.65,0.63,	**0.63**
b. April	0.62		**b**. Nov, Mar, April	0.55 0.54,	**0.53**	**Rain Season**		
Rain Season	0.62	**0.57**	**Rain Season**	0.53		**a**. May, June, July, Sept, Oct	0.63, 0.62	
a. May, June, Oct	0.57		a.June, July, Aug, Sept	0.51	**0.40**			
b. July, Aug, Sept.	0.54, 0.51, 0.55	**0.53**	**b.** May **c.** Oct	0.41, 0.40	**0.46** **0.56**	**b.** Aug	0.54**,** 0.53, 0.50**,**0.53,	**0.53** **0.48**
	0.45, 0.44 0.46	**0.45**		0.39, 0.40 0.46 0.56			0.53 0.48	
K_T Values								

Period	Kano		Period	Owerri		Period	Benin City	
	Ind.	**Ave**		Ind.	**Ave**		Ind.	**Ave**
Dry Season			**Dry Season**			**Dry Season**		
a. Nov, Dec,	0.62,		**a.** Nov, Dec,	0.56,		**a.** Nov, Dec,	0.55,	
Jan, Feb,	0.63		Jan	0.56,	**0.56**	Jan	0.55,	**0.5**
Mar, Apr	0.62,	**0.6**	**b.** Feb, Mar,	0.57		**b**. Feb, Mar,	0.56	**5**
Rain Season	0.63	**3**	Apr	0.51,	**0.52**	Apr	0.52,	
a.Oct, May	0.63,		**Rain Season**	0.53,		**Rain Season**	0.51,	**0.5**
June,	0.63		**a**. Aug, July,	0.52		**a.** July, Sept	0.50	**1**
b. July, Aug		**0.6**	Sept		**0.38**	**b.** June, Oct		
Sept	0.61,	**1**	**c.** June, Oct	0.36,	**0.45**	**c.** May	0.38,	**0.3**
	0.62		**d.** May	0.39,	**0.49**	**d.** Aug	0.37	**8**
	0.61	**0.5**		0.38			0.40,	**0.4**
	0.55,0.5	**4**		0.44,			0.42	**1**
	2			0.45			0.46	**0.4**
	0.56			0.49			0.34	**6**
								0.3
								4

The distribution curves of clearness index are plotted from the classification of the monthly average clearness index of Table 3 for each study location and are given in Fig 1 (a – f) for each study location. From Fig 1 (a – f), it is noted that the distribution curves of clearness index for all the study locations started from a low ordinate, though, not from the origin of the graph and steeply increased in value in a positive direction, indicating a steady increment in value of the solar radiation with fractional time. It is also observed that the distribution curves are clustered together for each study location and month. This is in agreement with the finding of Ref. [9] as the distribution curves of clearness index for the same locality is not much different.

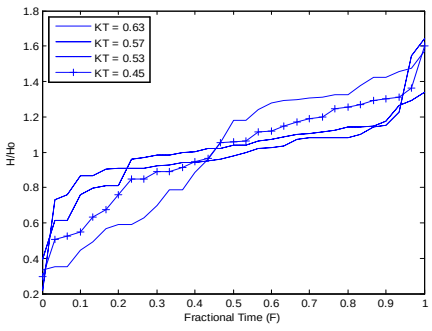

a. Abuja

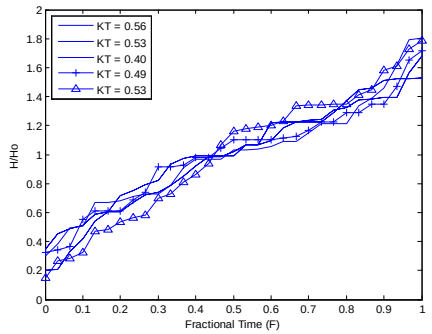

b. Lagos

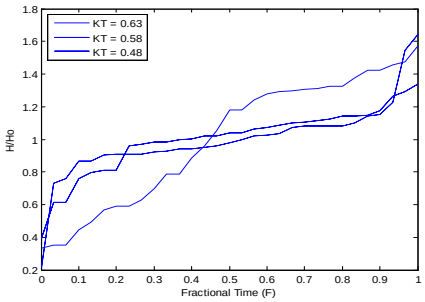

c. Bauchi

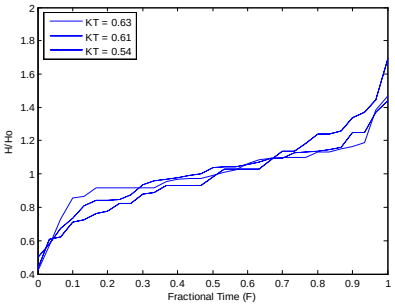

d. Kano

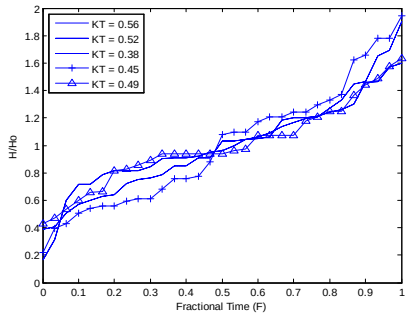

e. Owerri

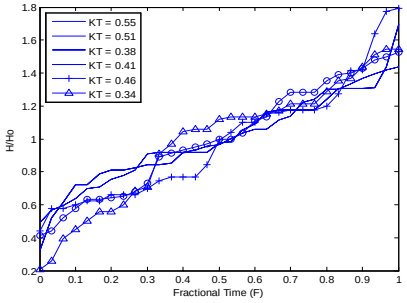

f. Benin City

Figures 1 (a – f) monthly distribution curves of clearness index for the study location

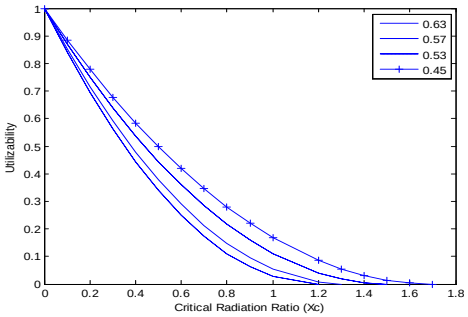

a. Abuja

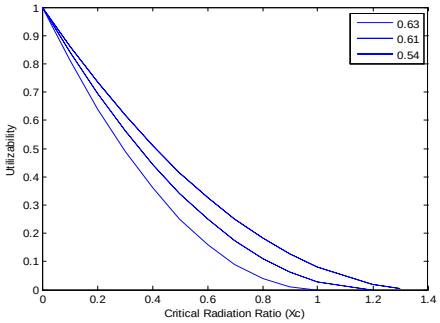

d. Kano

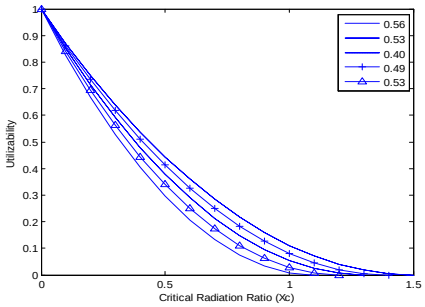

b. Lagos

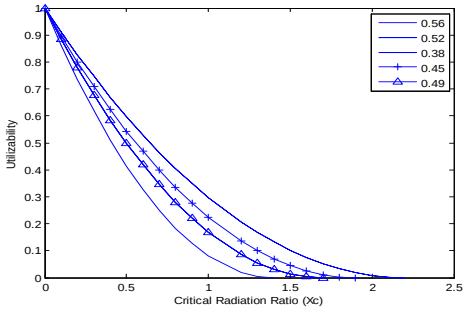

e. Owerri

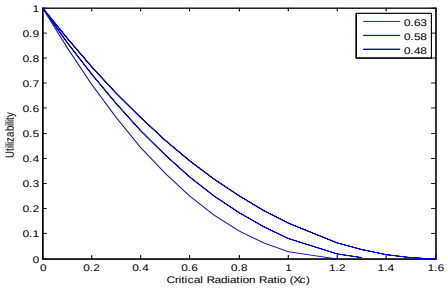

c. Bauchi

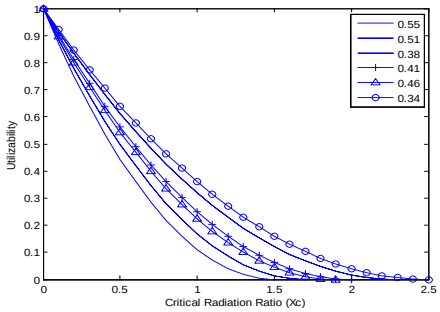

f. Benin City

Figure 2 (a – f) Utilizability curves for the study locations

The utilizability curves for the study locations are shown in Fig. 2 (a – f). It is observed from Fig 2 (a – f) that the utilizability curves spread out depending on the value of the clearness index. For a given location and values of monthly solar radiation, clearness index with lower values have their utilizability curves more spread out than those with higher values of clearness index. This reveals that the clearness index with higher values will yield higher values of solar radiation compared to those of lower values of clearness index. It is also worth noting that seasonal classification of

clearness index as given in Table 2 reveal that clearness index of higher values are the months of the dry season. Hence, this means that higher solar radiation utilizability value are expected during the months of the dry season than the wet seasons

IV. CONCLUSION

Evaluation of daily utilizability of flat plate solar collector on horizontal surface was carried out by the characterization of sky conditions of the study locations using clearness index determined from measured daily global solar radiation. The sky conditions of Abuja, Lagos and Bauchi were found to have four, five and three groupings, respectively, while, Kano, Owerri and Benin City had three, five and six sub-divisions, respectively. For each study location, distribution curves of clearness index were observed to cluster together which is in agreement with the findings of Ref [9]. Clearness index of lower value were observed to spread out more than those of higher value, indicating the possibility of harvesting more solar radiation in the months that contribute to the higher clearness index values. From the monthly K_T distribution curves, utilizability equations were generated for the plot of utilizability curves for each study location.

NOMENCLATURE

A_C Total Collector Area (m^2)
F_R Collector Heat Removal Factor
G_{sc} Solar Radiation Constant (W/m^2)
H Monthly Average Daily Global Solar Radiation on a Horizontal Surface (MJ/m^2)
H_o Monthly Extraterrestrial Radiation (MJ/m^2)
I_C Critical Radiation Level
$\bar{I}_m$ Monthly Average Solar Radiation on a Horizontal Surface
I Hourly Incident Global Solar Radiation on a Horizontal Surface (W/m^2)
K_T Clearness Index
q_{ab} Energy Absorb by Collector Area (W/m^2)
q_L Energy Loss by Collector (W)
q_u Useful Energy Gain by Collector (W)
Q_u Rate of Useful Energy Gain by Collector (MJ/m^2)
T_a Ambient Temperature (^oC)
T_{in} Fluid Inlet Temperature (^oC)
X_c Critical Solar Radiation Ratio
X_i Solar Radiation Ratio
f Fractional Time

Greek symbols

$\tau\alpha$ Transmissivity–Absorptivity Product
ϕ Utilizability
ω_s Hour Angle
δ Declination

REFERENCES

[1]. M.C.Njoku, I. Ofong, N.V. Ogueke, and E.E. - Anyanwu Characterization of Sky Conditions at Benin City and Owerri Nigeria. Journal of Fundamentals of Renewable Energy and Application. 2018, 8 (5), 1-8
[2]. Y.D. Goswami - Principles of Solar Engineering.: Taylor & Francis Group, CRC Press New York, 2015, ISBN 13: 978-1-4665-6379-7 (eBook-PDF)
[3]. H. Amir, Y. Ajabshirchi and A.A. Bakhtiar - Experimental analysis of flat plate solar air collector efficiency. Indian Journal of Science and Technology, 2012, 5 (8), 3183-3187
[4]. N.K.C. Sint, I. Choudhury, H.H. Masjuki and H. Aoyama - Theoretical Analysis to Determine the Efficiency of a CuO-water Nano-fluid Based-flat Plate Solar Collector for Domestic Solar Water Heating System in Myanmar, Solar Energy 2017, 155, 608–619
[5]. S. Fabio (2008) Analysis of a Flat Plate Solar Collector. Project Report MVK 160 Heat and Mass Transport.
[6]. S.A. Kalogirou - Solar Thermal Collectors and Applications. Energy and Combustion Science, 2004, 30, 231-295
[7]. S.A. Klein - Calculation of Flat Plate Collector Utilizability. Solar Energy, 1978 21 147-156
[8]. B.Y.H. Liu and R.C. Jordan - The Long Term Average Performance of Flat Plate Solar Collectors. Solar Energy, 1963, 7(2), 53-70
[9]. M.P.G. Sirimanna and R.A. Attalage - Estimation of Annual Collectable Energy on a Flat Plate Collector by Utilizability Concept: A Case Study of Colombo. Procedings of International Confrence on Energy and Sustainability.2013,1-5
[10]. A. Whillier - Solar Energy collection and its Utilization for House Heating. Ph.D. Thesis in Mechanical Engineering M.I.T. Cambridge, Massachusetts, **1953**
[11]. J.C. Theilacker and S.A. Klein - Improvements in Utilizability Relationships. ASME Journal of Solar Energy Engineering, 1980, p.271
[12]. Clark, D.R., Klein, S.A. and Beckman, W.A. (1983) Algorithm for Evaluating Hourly Radiation Utilizability Function. Journal of Solar Energy Engineering, 1983, 105/281, 1-7.
[13]. M. Collares-Pereira and A. Rabl - Simple Procedure for Predicting Long Term Average Performance of Non-Concentrating

and of Concentrating Solar Collector. Solar energy, 1979, 23, 235-253
[14]. H. Suehrcke and P.G. McCormick - (1989) Solar Radiation Utilizability. Solar Energy 1986, 43 (6), 339 - 345.
[15]. T.A. Reddy, S. Kumar and G.Y. Saunier - Review of Solar Radiation Analysis Techniques for Predicting Long-Term Thermal Collector Performance Applicability to Bangkok Data. Renewable Energy Review Journal, 1985, 7 (2), 56-80.
[16]. J.M. Gordon, D. Govaer and Y. Zarmi - The Utilizability Method with Hourly Vs Daily Insolation Data. Solar Energy, 1981, 27 (2), 99-102.
[17]. C. Armenta-Deu and M.C. De Andres - Correlation of a New Utilizability Function to Experimental Data for Southwestern Europe. Renewable Energy, 1991, 1 (5/6), 571-582.
[18]. Kiatsiriroat, T., Namprakai, P. and Hiranlabh, J. (1993) Performance Estimation of PV Water-Pumping System with Utilizability Function. John Wiley and Son, 1993, 305-310.
[19]. C.T. Leung, - The Utilizability Method of Predicting the long Term Performance of Flat-Plate Solar Collector. Renewable Energy Review Journal, 1982, 4 (2) 20-27.
[20]. J. Chndrasekaran and S. Kumar - Daily Utilizability from Hourly Cumulative Frequency Curves. Renewable Energy, 1994, 4 (8) 891-895.
[21]. B. Janarthanan, J. Chandrasekaran, and S. Kumar - Monthly Mean Daily Utilizability of South India. International Energy Journal, 2004, 5(1), 33-40.
[22]. R.K. Aruna and B. Janarthanan - Utilizability for Chennai, Trivandrum and Visakhapatnam. International Journal of Engineering and Innovative Technology, 2014, 3(12), 291-296
[23]. S. Ravichandran and J.D. Rathnaraj - Long Term Performance of Double Slope Tilted-Wick Type Solar Still – utilizability Function. Journal of Applied Sciences Research, 2015, 11(23), 47-50
[24]. W.A. Beckman (1998) Modern Computing Methods in Solar Energy Analysis. The Second ISES Europe Solar Congress, EuroSun 98, Book of Proceedings, 1988, 1, 1-11
[25]. J.A. Duffie and W.A. Beckman Solar Engineering of Thermal Processes. John Wiley & son, Inc USA. **2013**
[26]. ASHRAE - Solar domestic and service hot water manual (1983)
[27]. A. Kuye and S.S. Jagtap - Analysis of Solar Radiation Data for Port-Harcourt, Nigeria. Solar Energy, 1992, 49 (2), 139-145
[28]. F.J.K. Ideriah and S.O. Suleman - Sky conditions at Ibadan during 1975-1980. Solar Energy, 1989, 43 (6), 325-330
[29]. D.T. Reindl, W.A. Beckman and J.A. Duffie - Diffuse Fraction Correlations. Solar Energy, 1990, 45 (1), 1- 7
[30]. D.H.W. Li, and J.C. Lam - An Analysis of Climate Parameters and Sky Condition. Building and Environment, 2001, 36: 435 - 445
[31]. D.H.W. Li, C.C.S. Lau, and J.C. Lam - Overcast Sky Conditions and Luminance Distribution in Hong Kong. Building and Environment, 2004, 39: 101-108

Njoku M.C, et.al."Evaluation of Flat-Plate Solar Thermal Collector Daily Utilizability for Some Nigerian Cities" *International Journal of Engineering Research and Applications (IJERA*), vol.10 (02), 2020, pp 12-21.